

000 001 002 003 004 005 006 007 008 009 010 011 012 013 014 015 016 017 018 019 020 021 022 023 024 025 026 027 028 029 030 031 032 033 034 035 036 037 038 039 040 041 042 043 044 045 046 047 048 049 050 051 052 053 LEARNING FAST AND SLOW: ADDRESSING TASK-IMBALANCED CONTINUAL LEARNING WITH DECOUPLED DUAL-SPEED ADAPTATION

Anonymous authors

Paper under double-blind review

ABSTRACT

Continual learning aims to acquire new knowledge without forgetting previously learned tasks. However, most existing studies assume balanced tasks, which is rarely the practice case, as real-world scenarios often exhibit severe task imbalance with long-tailed distributions. This task-imbalanced continual learning (TICL) setting entangles two fundamental challenges: the well-known *stability–plasticity dilemma*, and the newly emerging *head–tail learning dilemma*, where head classes dominate training while tail classes remain under-optimized. To address this compounded difficulty, we propose Decoupled Fast–Slow Adaptation (DFSA), which introduces two key components. First, a fast–slow dual adapter augments the image encoder with a fast-adapting branch for rapid task acquisition and a slow-consolidating branch for stable knowledge retention. A task-modulated weighting mechanism dynamically integrates these branches, effectively fusing “fast” and “slow” thinking to balance short-term plasticity with long-term stability, while simultaneously providing complementary perspectives that enhance learning for underrepresented classes. Complementarily, DFSA employs a decoupled training strategy by first fine-tuning the text encoder as a semantic-aware classifier before updating image features, providing stable guidance that mitigates the negative impact of long-tailed distributions. Extensive experiments on TICL benchmarks show that our method significantly improves both few-sample task generalization and overall retention, outperforming existing continual learning baselines. The source code is temporarily available at <https://anonymous.4open.science/r/DFSA-3aD6E>.

1 INTRODUCTION

Human beings possess the remarkable ability to acquire new skills and adapt to evolving environments while retaining knowledge from past knowledge. Inspired by this, enabling deep models to achieve such continual learning (CL) (Wang et al., 2024a; Liu et al., 2025a) ability in artificial intelligence has been a long-standing goal, as it would allow models to operate robustly in dynamic and open-ended environments. Despite recent advances (Liu et al., 2025b; Wu et al., 2025; Huang et al., 2024; Liu et al., 2023; Thengane et al., 2022) driven by pre-trained foundation models such as CLIP (Radford et al., 2021), CL remains fundamentally constrained by the stability–plasticity dilemma: excessive plasticity causes catastrophic forgetting, while excessive stability impedes the acquisition of novel concepts.

The challenge becomes even more severe under real-world scenarios, where data typically follow a long-tailed distribution (Li et al., 2024; Zhang et al., 2023; Li et al., 2022) and arrive sequentially. In such cases, data streams often exhibit an extremely imbalanced (Hong et al., 2024; Liu et al., 2022): particular tasks contain abundant samples, whereas many others provide far fewer. To capture this more general and realistic setting, researchers have recently introduced task-imbalanced continual learning (TICL) (Hong et al., 2024). This imbalance introduces dual challenges, namely learning rare classes effectively while mitigating catastrophic forgetting. In essence, models in TICL are internally constrained by the stability–plasticity dilemma and externally challenged by the head–tail learning dilemma.

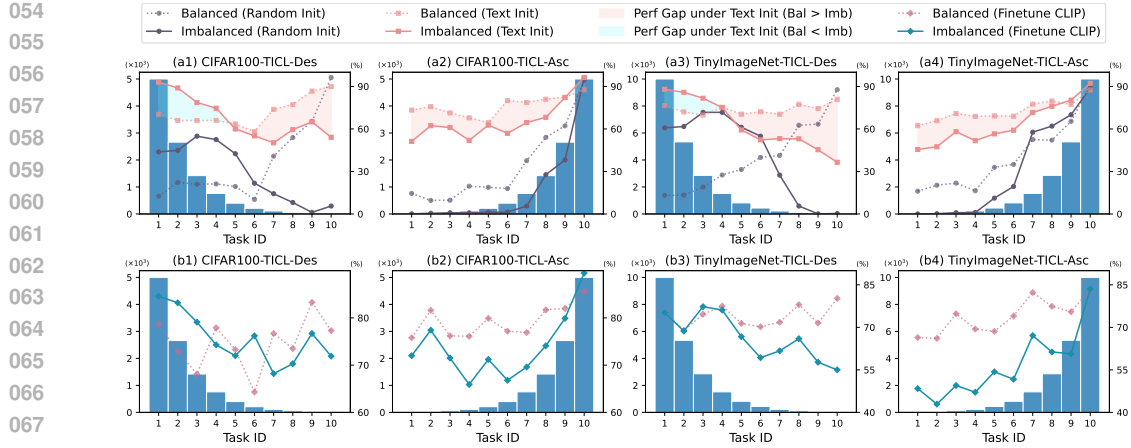


Figure 1: Final evaluation of the model on all learned tasks after sequential training. We conducted experiments on CIFAR100-TICL and TinyImageNet-TICL using classifiers (a1–a4) initialized either with text or randomly, as well as fine-tuning CLIP models (b1–b4).

Existing method joint training image representation and classifier (Hong et al., 2024; Liang & Li, 2024; Liu et al., 2023), or utilizing text guidance from the visual language models (Liu et al., 2025b; Yu et al., 2024; Zheng et al., 2023). However, training only the image encoder alongside a classifier often results in drastic performance drops on tail classes, as shown in Figure 1 (a1-a4), illustrating the intrinsic difficulty of learning under long-tailed distributions, and exhibiting patterns similar to those observed in regular long-tailed visual recognition (Shi et al., 2025; Li et al., 2023; Kang et al., 2020). More critically, certain tasks are almost completely forgotten across multiple classes (e.g., tasks 1–4 in Figure 1 a4). While methods incorporating the text encoder of visual-language models (VLMs) can alleviate part of the long-tail issue, they still struggle with pronounced imbalance. For example, in ascending distributions, early tail classes remain severely underrepresented and prone to catastrophic forgetting.

To address these joint challenges, we propose the Decoupled Fast–Slow Adaptation (DFSA) framework. Inspired by “Thinking, Fast and Slow” (Kahneman, 2011), DFSA introduces a Fast–Slow Adapter equipped with a task-modulated weighting mechanism that dynamically integrates a fast-adapting branch (analogous to Kahneman’s System 1) for rapid task acquisition and a slow-consolidating branch (analogous to System 2) for stable knowledge retention. This adaptive fusion allows both “fast” and “slow” knowledge to synergistically guide learning, improving overall task adaptation while mitigating catastrophic forgetting. It also provides complementary perspectives for each task, enhancing representations of under-sampled classes and mitigating long-tailed bias. Complementarily, DFSA leverages the unique structure of visual–language models through decoupled training. The text encoder, acting as a semantic-aware classifier, is fine-tuned before the image encoder. Since text features converge faster (Ma et al., 2025; Hentschel et al., 2022; Radford et al., 2021), this step provides stable guidance that reduces the negative impact of long-tailed distributions on underrepresented classes.

Extensive experiments demonstrate the effectiveness of DFSA in TICL, showing that it can achieve nearly comparable balanced performance across tasks in continual learning. Our main contributions are summarized as follows:

- To address the stability–plasticity dilemma, we propose the Fast–Slow Adapter, equipping the image encoder with a fast branch for rapid task adaptation and a slow branch for long-term consolidation. A task-modulated weighting mechanism dynamically fuses these branches, allowing fast and slow knowledge to guide learning and mitigate catastrophic forgetting synergistically.
- To mitigate the head–tail learning dilemma, DFSA employs a unique decoupled training strategy that first fine-tunes the text encoder of VLMs before updating image features. The rapidly converging text encoder effectively serves as a classifier, providing stable semantic guidance to calibrate subsequent image feature learning.
- By integrating the Fast–Slow Adapter with decoupled text-encoder training, DFSA achieves near-balanced continual learning performance across tasks, demonstrating strong effectiveness under task-imbalanced long-tailed scenarios.

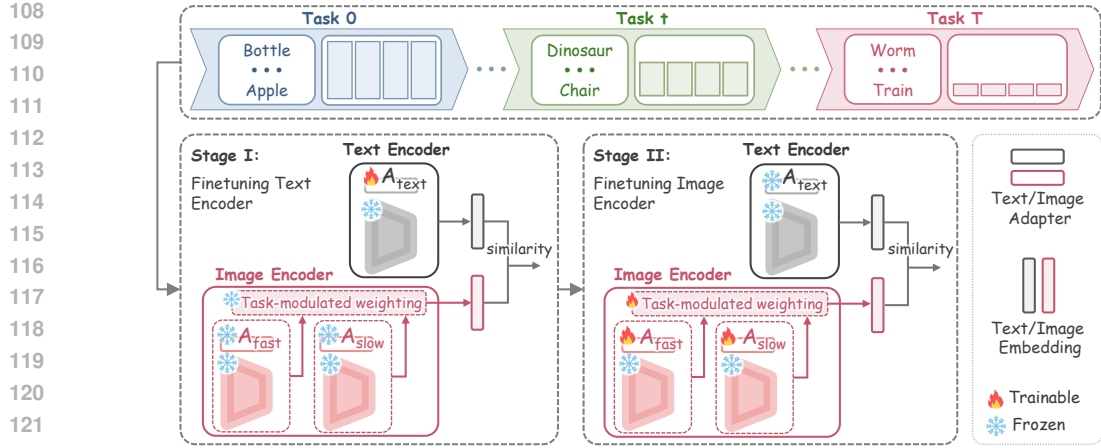


Figure 2: Training pipeline of DFSA, combining the Fast–Slow Adapter to alleviate the stability–plasticity dilemma and the decoupled training strategy to tackle the head–tail learning dilemma.

2 PROPOSED METHOD: DECOUPLED FAST–SLOW ADAPTATION

2.1 PRELIMINARIES

Problem Definition. We consider task-imbalanced continual learning (TICL), where the number of samples per task varies significantly throughout the learning process. In the conventional task-balanced continual learning setting with a sequence of $T+1$ tasks $\{\mathcal{D}_0, \mathcal{D}_1, \dots, \mathcal{D}_T\}$, each task \mathcal{D}_t contains N_t samples of equal size, i.e., $N_i = N_j, \forall i \neq j, i, j \in \{0, \dots, T\}$. In contrast, TICL relaxes this constraint and considers the more realistic scenario where task sizes follow a non-uniform distribution. Motivated by the long-tailed nature of real-world data and the setup in Hong et al. (2024), we assume that task sizes also follow a long-tailed distribution. Formally, let $\{I_0, I_1, \dots, I_T\}$ denote the task indices sorted in non-increasing order of size ($N_{I_0} > N_{I_1} > \dots > N_{I_T}$). Depending on the arrival order of tasks, TICL can manifest in three variants: *Descending (long-tailed) order*, tasks arrive as $\{I_0, I_1, \dots, I_T\}$, i.e., larger tasks first and smaller tasks later; *Ascending order*, tasks arrive in the reverse order $\{I_T, I_{T-1}, \dots, I_0\}$, i.e., smaller tasks first and larger tasks later; *Random order*, tasks arrive in a random permutation, independent of their sizes.

Parameter-Efficient Fine-Tuning (PEFT). Instead of updating all parameters of large vision-language models, PEFT techniques introduce lightweight trainable modules while keeping the pre-trained backbone frozen. Among them, LoRA (Hu et al., 2022), Adapter (Houlsby et al., 2019) and its variant AdaptFormer (Chen et al., 2022) are widely adopted. LoRA (Hu et al., 2022) constrains parameter updates to a low-rank subspace by decomposing $\Delta W \in \mathbb{R}^{m \times n}$ into AB with $A \in \mathbb{R}^{m \times r}$ and $B \in \mathbb{R}^{r \times n}$, where $r \ll \min(m, n)$, so that the updated layer becomes $h' = (W_0 + AB)x$ with W_0 frozen. Adapters (Houlsby et al., 2019) insert small bottleneck modules into each transformer block, mapping $h \in \mathbb{R}^d$ through a down-projection, nonlinearity, and up-projection as $h' = h + W_{\text{up}} \sigma(W_{\text{down}} h)$. AdaptFormer (Chen et al., 2022) further stabilizes adapters by adding a LayerNorm and a learnable scaling factor α , yielding $h' = h + \alpha \cdot W_{\text{up}} \sigma(W_{\text{down}} \text{LN}(h))$. In our framework, any of these can be employed to construct the Dual-Speed Adapter, allowing flexible and efficient adaptation.

2.2 DECOUPLED FAST–SLOW ADAPTATION

TICL presents two intertwined challenges: the stability–plasticity dilemma makes it difficult to retain past knowledge without sacrificing adaptation to new tasks, while the long-tailed distribution leads to biased representations that hurt underrepresented tasks. To address these challenges, we introduce the Fast–Slow Adapter, which combines a fast branch for rapid task adaptation with a slow branch for long-term knowledge consolidation. A task-modulated weighting mechanism dynamically fuses these branches, allowing their contributions to adapt per task. By ensuring that both fast-adapted and slow-consolidated knowledge are leveraged for each task, the model can better rep-

162 resent under-sampled (tail) classes, thereby mitigating the bias caused by long-tailed distributions
 163 while alleviating the stability–plasticity dilemma. To further reduce the impact of long-tailed dis-
 164 tributions, we adopt a decoupled learning strategy by fine-tuning the text encoder before updating
 165 the image encoder, leveraging the faster convergence and semantic reliability of text features. Inte-
 166 grating these components, we propose the Decoupled Fast–Slow Adaptation (DFSA) framework for
 167 effective TICL. The pipeline of DFSA is illustrated in Figure 2.

168 2.2.1 DUAL SPEED ADAPTER

170 Motivated by Kahneman’s dual-process theory (Kahneman, 2011), where “System 1” enables fast
 171 but short-lived adaptation and “System 2” supports slow but persistent consolidation, we design a
 172 dual-speed adaptation mechanism for the image encoder. In this analogy, the fast adapter plays the
 173 role of “System 1”, capturing rapid but transient adjustments, while the slow adapter corresponds to
 174 “System 2”, providing gradual and stable consolidation. Adapters are lightweight modules with only
 175 a small number of parameters (e.g., LoRA (Hu et al., 2022), Adapter (Houlsby et al., 2019), Adapt-
 176 Former (Chen et al., 2022)). We take the standard Adapter (Houlsby et al., 2019) as an example to
 177 illustrate the module design.

178 **Fast-Slow Adapter.** Building upon the standard adapter design, we extend it into two comple-
 179 mentary branches within the image encoder: a fast adapter and a slow adapter. The fast adapter
 180 enables rapid adaptation to new tasks by capturing task-specific patterns while leaving the base en-
 181 coder largely unchanged, whereas the slow adapter gradually consolidates knowledge to maintain
 182 long-term stability.

183 Given an input feature $h \in \mathbb{R}^d$, the standard adapter is formulated as

$$184 \text{Adapter}(h) = h + W_{\text{up}}\sigma(W_{\text{down}}h), \quad (1)$$

186 where $W_{\text{down}} \in \mathbb{R}^{r \times d}$, $W_{\text{up}} \in \mathbb{R}^{d \times r}$, and $\sigma(\cdot)$ denotes a non-linear activation. We extend this
 187 structure into two complementary branches with different adaptation speeds. The fast and slow
 188 branches are defined as

$$189 \text{A}_{\text{fast}}(h) = h + \alpha W_{\text{up}}^{\text{fast}} f(W_{\text{down}}^{\text{fast}} h), \quad \text{A}_{\text{slow}}(h) = h + \beta W_{\text{up}}^{\text{slow}} f(W_{\text{down}}^{\text{slow}} h), \quad (2)$$

191 where $\alpha > \beta$.

192 As shown in Figure 3, the accuracy of some tasks does not monotonically decrease. Instead, they
 193 occasionally improve after learning new tasks. This indicates that both past knowledge and current
 194 knowledge are beneficial, and their proper combination can lead to better performance. We introduce
 195 a task-modulated weighting strategy to dynamically balance the contributions of the fast and slow
 196 adapters. Given image features $F \in \mathbb{R}^{B \times d}$ for a batch of size B , we compute a task context as
 197 $c = \frac{1}{B} \sum_{i=1}^B F_i$, and obtain a modulating coefficient

$$198 \gamma = \sigma(\text{MLP}(c)) \in (0, 1), \quad (3)$$

200 where $\sigma(\cdot)$ is the sigmoid activation. Then, the final Fast–Slow Adapter is written as

$$201 \text{FSA}(h) = \gamma \cdot \text{A}_{\text{fast}}(h) + (1 - \gamma) \cdot \text{A}_{\text{slow}}(h). \quad (4)$$

203 The modulated coefficient γ is learned jointly with the Fast–Slow Adapter in an end-to-end manner.
 204 Both adapters are lightweight, introducing only a small number of trainable parameters, which al-
 205 lows the image encoder to rapidly adapt to new tasks through the fast adapter, while maintaining
 206 long-term stability via the slow adapter.

207 2.2.2 DECOUPLED LEARNING OF TEXT AND IMAGE ENCODER.

209 **Empirical Observation.** In TICL, the impact of long-tailed distributions is further amplified over
 210 sequential updates. First, *head-class bias* arises because the prevalence of head-class samples
 211 induces head-class dominance, resulting in biased decision boundaries and severely compressed
 212 tail-class representations. Second, *cumulative bias* emerges as this imbalance accumulates across
 213 tasks: in settings such as ascending or random orders, the skew compounds over time, leading to
 214 increasingly distorted feature spaces and catastrophic forgetting. To mitigate such issues, decoupled
 215 learning methods (Zhong et al., 2021; Kang et al., 2020; Zhou et al., 2020) in long-tailed visual
 recognition typically adopt a two-stage strategy by learning a feature representation first, and then

re-balancing the classifier with balanced data sampling. However, this paradigm is suboptimal for continual learning. As image feature representations $f(x)$ are sequentially updated with new tasks, a classifier trained on previous features becomes misaligned with the current feature space, causing significant catastrophic forgetting.

To empirically examine this issue, we compare two decouple learning strategies: first fine-tuning the image encoder (Img Enc) versus first fine-tuning the text encoder (Text Enc). The results, presented in Figure 3, demonstrate clear differences in stability and performance. These findings motivate the following observation.

Observation 1 (Feature Drift Amplifies Forgetting). *In continual learning, the sequential updates of image features $f(x)$ induce a mismatch between the classifier and the shifting feature space, causing decision boundary misalignment and consequently aggravating forgetting.*

This observation highlights the risk of feature drift. If the classifier is adjusted after feature updates, it will repeatedly fall out of alignment with the evolving representation space. To mitigate this issue, we adopt the opposite strategy. Instead of adapting the classifier to drifting features, we first fix a relatively balanced classifier that serves as a stable semantic reference. Subsequent image features are then encouraged to align with this reference, thereby reducing head-class dominance and alleviating forgetting. Building upon this intuition, we formalize the design principle in the following proposition.

Proposition 1 (Fast-first margin stabilization). *Updating the fast-converging component before the slow component establishes a stable semantic anchor across classes. This stabilizes the class-wise margins and reduces the risk of bias accumulation, thereby alleviating class imbalance and mitigating forgetting during sequential updates.*

Analysis. Let g denote the fast-converging component and f the slow component. Let μ_c be the feature prototype of class c , i.e., the mean of $f(x)$ over class- c samples.

When g is trained to near convergence, each $g(c)$ serves as a stable semantic anchor for class c . Subsequent updates to f adjust μ_c primarily to better align with $g(c)$. Because g is discriminative across classes, these updates: (1) Move each μ_c toward its own anchor $g(c)$; (2) Limit excessive separation between head and tail classes; (3) Reduce feature drift across sequential tasks.

A simple first-order analysis at the class prototype level shows that the expected update direction for each class c satisfies

$$\mathbb{E}[\Delta\mu_c] \propto g(c) - \mu_c + \epsilon_c,$$

where ϵ_c is a small residual due to inter-class interference. Since $g(c)$ is nearly fixed and discriminative, the residual is bounded and μ_c remains close to its anchor. Therefore, class-wise margins remain controlled, preventing uncontrolled drift or bias accumulation.

Fixing the fast-converging component first provides a reliable semantic reference. This guides the slow component to evolve its features in a stable and balanced manner, which reduces the risk of head-class dominance and mitigates forgetting during sequential updates. This analysis formalizes the intuition behind the fast-first design principle without requiring exact margin inequalities or heavy assumptions on tail classes. \square

Theorem 1 (Fast convergence of text encoder). *Under standard optimization settings, the text encoder converges faster than the image encoder.*

Proof Sketch. Text data are typically lower-dimensional and semantically more structured than image data (Ma et al., 2025; Radford et al., 2021; Yin et al., 2019). As a result, the corresponding encoder parameters reach a near-optimal solution in fewer gradient steps. Fixing this fast-converging

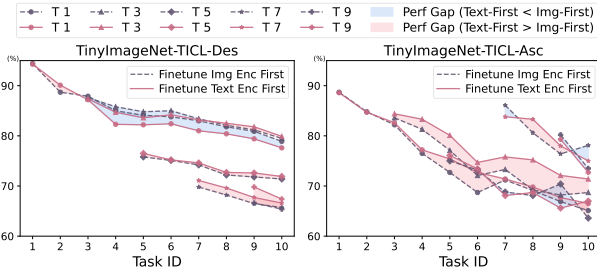


Figure 3: Accuracy evolution on 5 representative tasks (selected for clarity). Performance Gap (Perf Gap) shows text-first fine-tuning generally outperforms image-first, with occasional exceptions.

Observation 1 (Feature Drift Amplifies Forgetting). In continual learning, the sequential updates of image features $f(x)$ induce a mismatch between the classifier and the shifting feature space, causing decision boundary misalignment and consequently aggravating forgetting.

This observation highlights the risk of feature drift. If the classifier is adjusted after feature updates, it will repeatedly fall out of alignment with the evolving representation space. To mitigate this issue, we adopt the opposite strategy. Instead of adapting the classifier to drifting features, we first fix a relatively balanced classifier that serves as a stable semantic reference. Subsequent image features are then encouraged to align with this reference, thereby reducing head-class dominance and alleviating forgetting. Building upon this intuition, we formalize the design principle in the following proposition.

Proposition 1 (Fast-first margin stabilization). *Updating the fast-converging component before the slow component establishes a stable semantic anchor across classes. This stabilizes the class-wise margins and reduces the risk of bias accumulation, thereby alleviating class imbalance and mitigating forgetting during sequential updates.*

Analysis. Let g denote the fast-converging component and f the slow component. Let μ_c be the feature prototype of class c , i.e., the mean of $f(x)$ over class- c samples.

When g is trained to near convergence, each $g(c)$ serves as a stable semantic anchor for class c . Subsequent updates to f adjust μ_c primarily to better align with $g(c)$. Because g is discriminative across classes, these updates: (1) Move each μ_c toward its own anchor $g(c)$; (2) Limit excessive separation between head and tail classes; (3) Reduce feature drift across sequential tasks.

A simple first-order analysis at the class prototype level shows that the expected update direction for each class c satisfies

$$\mathbb{E}[\Delta\mu_c] \propto g(c) - \mu_c + \epsilon_c,$$

where ϵ_c is a small residual due to inter-class interference. Since $g(c)$ is nearly fixed and discriminative, the residual is bounded and μ_c remains close to its anchor. Therefore, class-wise margins remain controlled, preventing uncontrolled drift or bias accumulation.

Fixing the fast-converging component first provides a reliable semantic reference. This guides the slow component to evolve its features in a stable and balanced manner, which reduces the risk of head-class dominance and mitigates forgetting during sequential updates. This analysis formalizes the intuition behind the fast-first design principle without requiring exact margin inequalities or heavy assumptions on tail classes. \square

Theorem 1 (Fast convergence of text encoder). *Under standard optimization settings, the text encoder converges faster than the image encoder.*

Table 1: Comparison Results (%) on ImageNet-R-TICL.

Method	Descending		Ascending		Shuffled	
	$\overline{ACC} \uparrow$	$ACC \uparrow$	$\overline{ACC} \uparrow$	$ACC \uparrow$	$\overline{ACC} \uparrow$	$ACC \uparrow$
Pre+iCaRL (Rebuffi et al., 2017)	48.41	29.55	24.40	29.17	40.21	23.02
BiC (Wu et al., 2019)	21.91	18.9	13.52	16.01	16.3	16.32
PODNET (Douillard et al., 2020)	22.32	18.90	16.61	16.62	17.11	18.70
EEIL++ (Liu et al., 2022)	18.50	17.81	15.76	15.60	15.79	16.30
LUCIR++ (Liu et al., 2022)	18.36	21.29	8.05	8.27	15.62	15.62
Pre+FT (Khan et al., 2023)	40.60	7.68	18.22	21.15	21.37	22.62
Continual-CLIP (Thengane et al., 2022)	81.62	74.27	77.86	74.30	80.59	74.23
L2P (Wang et al., 2022b)	69.19	55.83	39.59	53.73	55.80	55.15
DualPrompt (Wang et al., 2022a)	65.99	51.03	38.03	51.43	50.01	50.65
CODA-Prompt (Smith et al., 2023)	73.98	60.72	42.33	59.15	58.19	58.37
DAP (Hong et al., 2024)	57.19	42.62	36.39	44.80	47.11	44.53
MoE-Adapters (Yu et al., 2024)	86.50	79.80	78.68	79.23	83.83	79.15
LoRA-DRS (Liu & Chang, 2025)	78.83	66.90	38.61	55.08	56.13	60.38
SD-LoRA (Wu et al., 2025)	77.29	66.75	50.67	65.07	65.86	66.18
DFSA (Ours)	87.66	81.37	80.78	79.68	84.58	80.67

component establishes stable class-wise embeddings, which then guide the slower-evolving image encoder to align its features accordingly. This reduces the risk of misalignment and mitigates forgetting without requiring explicit rebalancing at every step. \square

Detailed analysis is provided in Appendix A. According to Theorem 1 and Proposition 1, fine-tuning the text encoder first provides a reliable semantic anchor, guiding the subsequent learning of image features and mitigating feature drift across sequential tasks.

3 EXPERIMENTS

3.1 EXPERIMENTAL SETUP

Datasets and Evaluation Metrics. We evaluate our approach on three widely used benchmarks: CIFAR100-TICL, TinyImageNet-TICL, and ImageNet-R-TICL, which are derived from the original CIFAR100 (Krizhevsky et al., 2009), TinyImageNet (Le & Yang, 2015), and ImageNet-R (Hendrycks et al., 2021), respectively. CIFAR100 contains 100 classes with 500 images per class, while TinyImageNet contains 200 classes with 500 images per class sampled from ImageNet (Russakovsky et al., 2015). ImageNet-R includes 200 classes rendered in diverse artistic styles such as cartoons, graffiti, and origami, providing a challenging out-of-distribution variant of ImageNet.

Following the TICL protocol introduced by Hong et al. (2024), each dataset is restructured into a long-tailed variant and further divided into 10 disjoint tasks, forming their TICL counterparts: CIFAR100-TICL, TinyImageNet-TICL, and ImageNet-R-TICL. The data distribution of TICL is shown in Appendix B. TICL simulates more realistic incremental learning under long-tailed data distributions by considering three task-arrival scenarios: (1) *TICL-Descending*, where tasks arrive from head-class rich (data-abundant) to tail-class dominated (data-scarce); (2) *TICL-Ascending*, where tasks arrive in the reverse order, i.e., from tail to head; (3) *TICL-Shuffled*, where tasks arrive in a random sequence.

To assess model performance, we adopt two standard continual learning metrics: (1) *Average accuracy* (\overline{ACC}), which averages the accuracy over all encountered tasks at each training step, providing a more fine-grained measure of continual performance throughout learning; and (2) *Accuracy after the last stage* (ACC), which measures the accuracy on all tasks after the final task is learned, reflecting the overall effectiveness of sequential training. More specifically, let ACC_t denote the accuracy of the model after completing the t -th task. $\overline{ACC} = \frac{1}{T} \sum_{t=1}^T ACC_t$, and $ACC = ACC_T$.

State-of-the-art Methods. We compare the proposed DFSA against state-of-the-art approaches based on fine-tuning pre-trained models. (1) *Rehearsal-based methods*: PODNET (Douillard et al.,

Table 2: Comparison Results (%) on CIFAR100-TICL.

Method	Descending		Ascending		Shuffled	
	ACC ↑					
Pre+iCaRL (Rebuffi et al., 2017)	53.00	28.73	41.70	26.88	48.62	31.02
BiC (Wu et al., 2019)	27.92	38.02	36.08	37.90	27.11	33.63
PODNET (Douillard et al., 2020)	26.48	23.82	32.31	28.24	28.49	26.21
EEIL++ (Liu et al., 2022)	31.49	38.24	35.93	37.85	31.63	39.31
LUCIR++ (Liu et al., 2022)	27.71	21.26	42.39	28.92	35.62	25.94
Pre+FT (Khan et al., 2023)	65.83	22.02	19.52	25.58	43.30	33.56
Continual-CLIP (Thengane et al., 2022)	76.35	66.69	75.88	66.62	76.52	66.64
L2P (Wang et al., 2022b)	79.43	57.41	47.22	50.61	59.13	53.91
DualPrompt (Wang et al., 2022a)	81.76	63.21	54.96	50.96	65.22	57.21
CODA-Prompt (Smith et al., 2023)	78.09	51.65	58.20	53.19	69.08	61.58
DAP (Hong et al., 2024)	81.15	65.48	50.29	46.43	56.32	55.27
MoE-Adapters (Yu et al., 2024)	84.05	75.53	78.59	74.61	82.12	74.11
DFSA (Ours)	85.43	76.91	81.28	75.96	83.57	75.65
LoRA-DRS ¹ (Liu & Chang, 2025)	91.69	83.37	75.99	76.21	84.84	78.02
SD-LoRA ¹ (Wu et al., 2025)	88.42	76.64	73.20	72.34	81.41	72.93

Table 3: Comparison Results (%) on TinyImageNet-TICL.

Method	Descending		Ascending		Shuffled	
	ACC ↑					
L2P (Wang et al., 2022b)	82.98	64.45	60.14	59.56	66.28	61.34
DualPrompt (Wang et al., 2022a)	81.53	60.17	58.16	61.71	66.31	60.82
CODA-Prompt (Smith et al., 2023)	80.79	59.28	64.81	61.14	71.98	61.74
DAP (Hong et al., 2024)	80.24	61.95	54.27	58.92	65.78	59.91
Continual-CLIP (Thengane et al., 2022)	74.69	65.92	73.39	65.94	74.38	65.95
MoE-Adapters (Yu et al., 2024)	81.75	72.92	76.31	72.29	78.88	72.24
DFSA (Ours)	83.24	74.12	77.47	73.16	80.11	73.48
LoRA-DRS ¹ (Liu & Chang, 2025)	84.64	72.54	67.40	51.09	75.43	64.01
SD-LoRA ¹ (Wu et al., 2025)	90.77	81.16	81.00	78.83	85.44	79.98

2020), and BiC (Wu et al., 2019), which are classical continual learning baselines. (2) *Long-tailed extensions*: EEIF++ (Liu et al., 2022) and LUCIR++ (Liu et al., 2022), designed to address class imbalance in continual learning. (3) *ViT-based methods*: L2P (Wang et al., 2022b), DualPrompt (Wang et al., 2022a), CODA-Prompt (Smith et al., 2023), FineTune (Khan et al., 2023), and DAP (Hong et al., 2024), which exploit prompt tuning (Jia et al., 2022) for task adaptation, as well as LoRA-based methods such as LoRA-DRS (Liu & Chang, 2025) and SD-LoRA (Wu et al., 2025). (4) *CLIP-based methods*: Continual-CLIP (Thengane et al., 2022), which leverages CLIP’s zero-shot generalization in TICL, and MoE-Adapters (Yu et al., 2024), which employ mixture-of-experts adapters for continual learning. (5) Other pre-trained baselines: FineTune (Khan et al., 2023) and iCaRL (Rebuffi et al., 2017) with pre-trained ViT.

Implementation Details. As a widely adopted representative of VLMs (Yu et al., 2024; Huang et al., 2024), we exploit CLIP as our backbone, specifically the ViT-B/16 version. We fine-tune both its image and text encoders using Adapter (Houlsby et al., 2019) as the PEFT technology. For all datasets, the adaptation rates mentioned in Section 2.2.1 are set as $\alpha = 0.5$ for the fast branch and $\beta = 0.1$ for the slow branch.

3.2 COMPARISON RESULTS

Tables 1 to 3 present the results of different methods on ImageNet-R-TICL, CIFAR100-TICL and TinyImageNet-TICL. The comparison results demonstrate the consistent superiority of DFSA over

¹The pre-training dataset is ImageNet-21K (Russakovsky et al., 2015; Ridnik et al., 2021), which overlaps with CIFAR100-TICL and TinyImageNet-TICL, potentially causing data leakage (Shi et al., 2024). Results on these benchmarks are therefore reported for reference only.

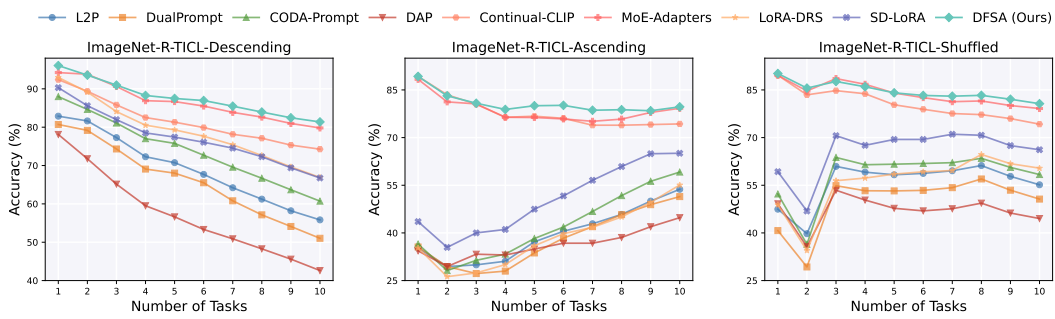


Figure 4: Average accuracy on all encountered tasks after sequential training on ImageNet-R-TICL.

Table 4: Ablation Results (%) on TinyImageNet-TICL. “Image-Text” updates the image encoder before the text encoder, while “Text-Image” indicates the reverse.

Decoupled Learning		FSA	Descending		Ascending		Shuffled	
			$\overline{ACC} \uparrow$	$ACC \uparrow$	$\overline{ACC} \uparrow$	$ACC \uparrow$	$\overline{ACC} \uparrow$	$ACC \uparrow$
✓	✗	✗	81.69	72.51	76.72	70.85	79.17	72.09
✗	✓	✗	82.52	73.08	77.01	72.64	79.85	72.37
✓	✗	✓	82.53	73.62	77.25	72.00	79.02	72.40
✗	✓	✓	83.24	74.12	77.47	73.16	80.11	73.48

state-of-the-art baselines. On ImageNet-R-TICL, DFSA achieves substantial improvements, surpassing recent strong baselines by over 10% in both \overline{ACC} and ACC . Notably, compared to SD-LoRA (with a ViT-B/16-IN21K backbone), DFSA achieves remarkable gains under the Ascending order (+30.11% \overline{ACC} and +14.61% ACC), showing its strong adaptability and stability. Against MoE-Adapters (a CLIP-based method), DFSA also delivers steady improvements, such as a +2.1% gain in \overline{ACC} under Ascending. On CIFAR100-TICL and TinyImageNet-TICL, DFSA further outperforms all compared methods (except methods with ViT-B/16-IN21K backbone) across all task orders. In particular, on CIFAR100-TICL, DFSA improves upon MoE-Adapters by more than 1.3% in every scenario, with \overline{ACC} gains reaching +2.69% under Ascending order. Consistent gains are also observed on TinyImageNet-TICL. Although SD-LoRA and LoRA-DRS are excluded from the comparisons due to pretraining overlap with ImageNet-21K, DFSA still surpasses them in several cases. For instance, on CIFAR100-TICL Ascending, DFSA outperforms LoRA-DRS and SD-LoRA by +5.29% and +8.08% in \overline{ACC} , respectively.

Figure 4 shows the sequential performance of various methods on ImageNet-R-TICL. In the Descending scenario, where head tasks arrive first, all methods start strong but gradually decline due to forgetting and underrepresented of tail tasks. DFSA declines the slowest, showing its superior robustness against forgetting. In the Ascending scenario, initial tasks have few samples, causing most methods to perform poorly initially. The arrival of larger tasks with richer samples leads to higher performance on these tasks, thereby raising the average accuracy. DFSA effectively leverages textual guidance to maintain strong performance throughout. Compared with MoE-Adapters, which also use textual information, DFSA exhibits a smoother accuracy curve, demonstrating its enhanced ability to mitigate catastrophic forgetting under extreme data scarcity. Additional results on CIFAR100-TICL and TinyImageNet-TICL are provided in Appendix C. Appendix D presents a comparison of per-task performance after training the final task.

3.3 ABLATION STUDY

Table 4 presents the ablation results evaluating the contributions of individual DFSA components. When decoupling the learning of text and image encoders, the Text-Image order consistently outperforms Image-Text, with a notable +1.79% ACC gain under the Ascending scenario, demonstrating that stabilizing the decision boundary before feature refinement is crucial for long-tailed tasks. Adding the Fast-Slow Adapter further boosts performance. Image-Text can also benefit from the Fast-Slow Adapter (FSA) in both Descending and Ascending, while in Shuffled it incurs only a marginal drop of 0.15% in ACC . Finally, combining Text-Image with the FSA yields the best results across all scenarios, underscoring the complementary roles of both components in DFSA.

432 4 RELATED WORK

434 **Continual Learning (CL).** Existing CL approaches primarily seek to mitigate catastrophic forgetting
 435 under the assumption of balanced task distributions and can broadly be categorized into three
 436 main types (Wang et al., 2024a; De Lange et al., 2021): architecture-based, regularization-based,
 437 and rehearsal-based methods. Architecture-based methods (Mallya et al., 2018; Rypešć et al., 2023;
 438 Li et al., 2025) adjust the model architecture and allocate specific parameters for different tasks.
 439 Regularization-based methods (Dhar et al., 2019; Lee et al., 2019; Zenke et al., 2017; Kirkpatrick
 440 et al., 2017) restrict parameter optimization by knowledge distillation or adding a penalty in the
 441 loss function, thus accommodating both previous and new tasks. Rehearsal-based methods (Rebuffi
 442 et al., 2017; Rolnick et al., 2019; Kumari et al., 2022) mitigate forgetting by replaying original or
 443 synthesized samples from previous tasks, which typically results in additional memory overhead and
 potential privacy risks.

444 **Fine-tuning Pre-trained Model for CL.** Recently, fine-tuning pre-trained models using parameter-
 445 efficient fine-tuning (PEFT) methods (Jia et al., 2022; Chen et al., 2022; Hu et al., 2022) has shown
 446 strong performance in CL. Some CL methods, such as L2P (Wang et al., 2022b), DualPrompt (Wang
 447 et al., 2022a) and CODA-Prompt (Smith et al., 2023) combined pre-trained Vision Transformer
 448 (ViT) (Dosovitskiy et al., 2021) with prompt tuning (Lester et al., 2021; Li & Liang, 2021). Ad-
 449 ditionally, several methods, like InflLoRA (Liang & Li, 2024) and SD-LoRA (Wu et al., 2025),
 450 fine-tune pre-trained ViT using LoRA (Hu et al., 2022) for CL. CLIP (Radford et al., 2021) con-
 451 tains knowledge from both the language and vision modalities and exhibits strong CL performance
 452 under zero-shot evaluation (Thengane et al., 2022). Liu et al. (2023) fine-tunes the image encoder
 453 using an adapter and preserves previous knowledge through a parameter retention mechanism and
 454 knowledge distillation. RAPF (Huang et al., 2024) also employs an adapter to adjust image features
 455 with a decomposed parameter fusion strategy to enhance stability, and utilizes textual information to
 456 separate neighboring categories. Yu et al. (2024) employs mixture-of-experts Adapters to fine-tune
 457 the image and text encoders of CLIP, and integrates the outputs of experts based on the input sample.

458 **Imbalanced Continual Learning.** This setting is characterized by two intertwined challenges:
 459 catastrophic forgetting and data imbalance, which exacerbate each other. Earlier research, such as
 460 BiC (Wu et al., 2019) and PRS (Kim et al., 2020), focuses on imbalanced continual learning based
 461 on sample rehearsal. Liu et al. (2022) defined long-tailed class-incremental learning (LT-CIL) and
 462 proposed a rehearsal-based two-stage approach. Some studies (He, 2024; Wang et al., 2024b) miti-
 463 gated the impact of data imbalance under LT-CIL (Liu et al., 2022). Recently, Hong et al. identified
 464 the challenges posed by task-level sample imbalance and introduced Task Imbalanced Continual
 465 Learning (TICL). In TICL, the sample sizes across tasks follow a long-tailed distribution, encom-
 466 passing three scenarios: Descending, Ascending, and Shuffled TICL. DAP (Hong et al., 2024), a
 467 rehearsal-free two-stage method, learned task-specific prompts in the first stage, and then integrated
 468 them into a general prompt in the second stage according to task sizes. While this method effec-
 469 tively tackled the challenges in TICL, its performance still remains inadequate. This paper focuses
 470 on task-level imbalance and aims to further improve the performance of three scenarios of TICL.

471 5 CONCLUSION

472 In this work, we proposed the Decoupled Fast-Slow Adaptation (DFSA) framework to address the
 473 compounded challenges of task-imbalanced continual learning. By combining a Fast-Slow Adapter
 474 with a task-modulated weighting mechanism, DFSA effectively balances short-term plasticity and
 475 long-term stability, while also providing complementary perspectives that benefit underrepresented
 476 tail classes. In addition, the decoupled training strategy leverages the semantic guidance of text
 477 encoders to further reduce the adverse effects of long-tailed distributions. Extensive experiments
 478 across multiple benchmarks demonstrate that DFSA consistently outperforms state-of-the-art meth-
 479 ods in both generalization to few-sample tasks and long-term knowledge retention.

480 Although DFSA demonstrates strong performance in TICL, its fast and slow adaptation speeds are
 481 manually set, which may not be optimal for all tasks. Future work will explore an automatic learn-
 482 ing strategy for these adaptation speeds to better handle heterogeneous tasks. Moreover, while
 483 TICL settings better reflect real-world scenarios than traditional task-balanced assumptions, more
 484 challenging conditions, such as highly non-stationary or cross-domain distributions, remain under-
 485 explored. Extending DFSA to these settings could further improve robustness and generalization in
 486 practical continual learning.

486 ETHICS STATEMENT
487488 Our research focuses on effectively alleviating the plasticity and stability dilemma and the newly
489 head-tail learning problem in TICL with the proposed DFSA, more applicable to real-world scenar-
490 ios where task streams arrive continuously and task sizes follow long-tailed distributions. We have
491 carefully considered the potential social impacts and anticipate no direct, immediate, or adverse
492 consequences. We are committed to the ethical dissemination of our research and to encouraging its
493 responsible use.494
495 REPRODUCIBILITY STATEMENT
496497 All the results in this work are reproducible. We provide a temporary code in the supplemental
498 materials and an anonymous repository linked in the Abstract to replicate our results. The repository
499 includes environment configurations, run scripts, and other relevant materials. A complete version
500 of the code will be released at a later stage. We discuss the experimental settings in Section 3.1,
501 including implementation details such as the backbone and the configuration of PEFT technology.502
503 REFERENCES
504505 Shoufa Chen, Chongjian Ge, Zhan Tong, Jiangliu Wang, Yibing Song, Jue Wang, and Ping Luo.
506 Adaptformer: Adapting vision transformers for scalable visual recognition. *NeurIPS*, 35:16664–
507 16678, 2022.508 Matthias De Lange, Rahaf Aljundi, Marc Masana, Sarah Parisot, Xu Jia, Aleš Leonardis, Gregory
509 Slabaugh, and Tinne Tuytelaars. A continual learning survey: Defying forgetting in classification
510 tasks. *IEEE TPAMI*, 44(7):3366–3385, 2021.512 Prithviraj Dhar, Rajat Vikram Singh, Kuan-Chuan Peng, Ziyan Wu, and Rama Chellappa. Learning
513 without memorizing. In *CVPR*, pp. 5138–5146, 2019.515 Alexey Dosovitskiy, Lucas Beyer, Alexander Kolesnikov, Dirk Weissenborn, Xiaohua Zhai, Thomas
516 Unterthiner, Mostafa Dehghani, Matthias Minderer, Georg Heigold, Sylvain Gelly, Jakob Uszko-
517 reit, and Neil Houlsby. An image is worth 16x16 words: Transformers for image recognition at
518 scale. In *ICLR*, 2021.519 Arthur Douillard, Matthieu Cord, Charles Ollion, Thomas Robert, and Eduardo Valle. Podnet:
520 Pooled outputs distillation for small-tasks incremental learning. In *ECCV*, pp. 86–102. Springer,
521 2020.523 Jiangpeng He. Gradient reweighting: Towards imbalanced class-incremental learning. In *CVPR*,
524 pp. 16668–16677, June 2024.525 Dan Hendrycks, Steven Basart, Norman Mu, Saurav Kadavath, Frank Wang, Evan Dorundo, Rahul
526 Desai, Tyler Zhu, Samyak Parajuli, Mike Guo, et al. The many faces of robustness: A critical
527 analysis of out-of-distribution generalization. In *CVPR*, pp. 8340–8349, 2021.529 Simon Hentschel, Konstantin Kobs, and Andreas Hotho. Clip knows image aesthetics. *Frontiers in
530 Artificial Intelligence*, 5:976235, 2022.532 Chenxing Hong, Yan Jin, Zhiqi Kang, Yizhou Chen, Mengke Li, Yang Lu, and Hanzi Wang.
533 Dynamically anchored prompting for task-imbalanced continual learning. *arXiv preprint
arXiv:2404.14721*, 2024.535 Neil Houlsby, Andrei Giurgiu, Stanislaw Jastrzebski, Bruna Morrone, Quentin De Laroussilhe, An-
536 drea Gesmundo, Mona Attariyan, and Sylvain Gelly. Parameter-efficient transfer learning for nlp.
537 In *ICML*, pp. 2790–2799, 2019.538 Edward J Hu, Yelong Shen, Phillip Wallis, Zeyuan Allen-Zhu, Yuanzhi Li, Shean Wang, Lu Wang,
539 and Weizhu Chen. Lora: Low-rank adaptation of large language models. In *ICLR*, 2022.

540 Linlan Huang, Xusheng Cao, Haori Lu, and Xialei Liu. Class-incremental learning with clip: Adaptive
 541 representation adjustment and parameter fusion. In *ECCV*, pp. 214–231. Springer, 2024.

542

543 Menglin Jia, Luming Tang, Bor-Chun Chen, Claire Cardie, Serge Belongie, Bharath Hariharan, and
 544 Ser-Nam Lim. Visual prompt tuning. In *ECCV*, pp. 709–727. Springer, 2022.

545 Daniel Kahneman. *Thinking, fast and slow*. Farrar, Straus and Giroux, 2011.

546

547 Bingyi Kang, Saining Xie, Marcus Rohrbach, Zhicheng Yan, Albert Gordo, Jiashi Feng, and Yannis
 548 Kalantidis. Decoupling representation and classifier for long-tailed recognition. In *ICLR*, 2020.

549 Muhammad Gul Zain Ali Khan, Muhammad Ferjad Naeem, Luc Van Gool, Didier Stricker, Federico
 550 Tombari, and Muhammad Zeshan Afzal. Introducing language guidance in prompt-based
 551 continual learning. In *ICCV*, pp. 11463–11473, 2023.

552

553 Chris Dongjoo Kim, Jinseo Jeong, and Gunhee Kim. Imbalanced continual learning with partitioning
 554 reservoir sampling. In *ECCV*, pp. 411–428. Springer, 2020.

555 James Kirkpatrick, Razvan Pascanu, Neil Rabinowitz, Joel Veness, Guillaume Desjardins, Andrei A
 556 Rusu, Kieran Milan, John Quan, Tiago Ramalho, Agnieszka Grabska-Barwinska, et al. Overcom-
 557 ing catastrophic forgetting in neural networks. *Proceedings of the national academy of sciences*,
 558 114(13):3521–3526, 2017.

559

560 Alex Krizhevsky, Geoffrey Hinton, et al. Learning multiple layers of features from tiny images.
 561 *Tech Report*, 2009.

562 Lilly Kumari, Shengjie Wang, Tianyi Zhou, and Jeff A Bilmes. Retrospective adversarial replay for
 563 continual learning. *NeurIPS*, 35:28530–28544, 2022.

564 Yann Le and Xuan Yang. Tiny imagenet visual recognition challenge. *CS 231N*, 7(7):3, 2015.

565

566 Kibok Lee, Kimin Lee, Jinwoo Shin, and Honglak Lee. Overcoming catastrophic forgetting with
 567 unlabeled data in the wild. In *ICCV*, pp. 312–321, 2019.

568

569 Brian Lester, Rami Al-Rfou, and Noah Constant. The power of scale for parameter-efficient prompt
 570 tuning. *arXiv preprint arXiv:2104.08691*, 2021.

571 Hongbo Li, Sen Lin, Lingjie Duan, Yingbin Liang, and Ness Shroff. Theory on mixture-of-experts
 572 in continual learning. In *ICLR*, 2025.

573

574 Mengke Li, Yiu-ming Cheung, and Yang Lu. Long-tailed visual recognition via gaussian clouded
 575 logit adjustment. In *CVPR*, pp. 6929–6938, 2022.

576 Mengke Li, Yiu-Ming Cheung, and Zhikai Hu. Key point sensitive loss for long-tailed visual recog-
 577 nition. *IEEE TPAMI*, 45(4):4812–4825, 2023.

578

579 Mengke Li, Ye Liu, Yang Lu, Yiqun Zhang, Yiu-ming Cheung, and Hui Huang. Improving vi-
 580 sual prompt tuning by gaussian neighborhood minimization for long-tailed visual recognition. In
 581 *NeurIPS*, volume 37, pp. 103985–104009, 2024.

582

583 Xiang Lisa Li and Percy Liang. Prefix-tuning: Optimizing continuous prompts for generation. *arXiv
 preprint arXiv:2101.00190*, 2021.

584

585 Yan-Shuo Liang and Wu-Jun Li. Inflora: Interference-free low-rank adaptation for continual learn-
 586 ing. In *CVPR*, pp. 23638–23647, 2024.

587

588 Wenzhuo Liu, Xin-Jian Wu, Fei Zhu, Ming-Ming Yu, Chuang Wang, and Cheng-Lin Liu. Class
 589 incremental learning with self-supervised pre-training and prototype learning. *PR*, 157:110943,
 2025a.

590

591 Wenzhuo Liu, Fei Zhu, Longhui Wei, and Qi Tian. C-CLIP: multimodal continual learning for
 592 vision-language model. In *ICLR*, 2025b.

593

Xialei Liu, Yu-Song Hu, Xu-Sheng Cao, Andrew D Bagdanov, Ke Li, and Ming-Ming Cheng. Long-
 tailed class incremental learning. In *ECCV*, pp. 495–512. Springer, 2022.

594 Xialei Liu, Xusheng Cao, Haori Lu, Jia-wen Xiao, Andrew D Bagdanov, and Ming-Ming
 595 Cheng. Class incremental learning with pre-trained vision-language models. *arXiv preprint*
 596 *arXiv:2310.20348*, 2023.

597 Xuan Liu and Xiaobin Chang. Lora subtraction for drift-resistant space in exemplar-free continual
 598 learning. In *CVPR*, pp. 15308–15318, 2025.

600 Shuailei Ma, Kecheng Zheng, Ying Wei, Wei Wu, Fan Lu, Yifei Zhang, Chen-Wei Xie, Biao Gong,
 601 Jiapeng Zhu, and Yujun Shen. Learning visual generative priors without text. In *CVPR*, pp.
 602 8051–8061, 2025.

603 Arun Mallya, Dillon Davis, and Svetlana Lazebnik. Piggyback: Adapting a single network to mul-
 604 tiple tasks by learning to mask weights. In *ECCV*, September 2018.

606 Alec Radford, Jong Wook Kim, Chris Hallacy, Aditya Ramesh, Gabriel Goh, Sandhini Agarwal,
 607 Girish Sastry, Amanda Askell, Pamela Mishkin, Jack Clark, et al. Learning transferable visual
 608 models from natural language supervision. In *ICML*, pp. 8748–8763, 2021.

609 Sylvestre-Alvise Rebuffi, Alexander Kolesnikov, Georg Sperl, and Christoph H Lampert. icarl:
 610 Incremental classifier and representation learning. In *CVPR*, pp. 2001–2010, 2017.

612 Tal Ridnik, Emanuel Ben Baruch, Asaf Noy, and Lihi Zelnik. Imagenet-21k pretraining for the
 613 masses. In *NeurIPS*, 2021.

615 David Rolnick, Arun Ahuja, Jonathan Schwarz, Timothy Lillicrap, and Gregory Wayne. Experience
 616 replay for continual learning. *NeurIPS*, 32, 2019.

617 Olga Russakovsky, Jia Deng, Hao Su, Jonathan Krause, Sanjeev Satheesh, Sean Ma, Zhiheng
 618 Huang, Andrej Karpathy, Aditya Khosla, Michael Bernstein, Alexander C. Berg, and Li Fei-Fei.
 619 Imagenet large scale visual recognition challenge. *IJCV*, 115(3):211–252, 2015.

621 Grzegorz Rypeś, Sebastian Cygert, Valeriya Khan, Tomasz Trzcinski, Bartosz Michał Zieliński,
 622 and Bartłomiej Twardowski. Divide and not forget: Ensemble of selectively trained experts in
 623 continual learning. In *ICLR*, 2023.

624 Jiang-Xin Shi, Tong Wei, Zhi Zhou, Jie-Jing Shao, Xin-Yan Han, and Yu-Feng Li. Long-tail learning
 625 with foundation model: Heavy fine-tuning hurts. In *ICML*, 2024.

627 Jiang-Xin Shi, Tong Wei, and Yu-Feng Li. Lift+: Lightweight fine-tuning for long-tail learning.
 628 *arXiv preprint arXiv:2504.13282*, 2025.

630 James Seale Smith, Leonid Karlinsky, Vyshnavi Gutta, Paola Cascante-Bonilla, Donghyun Kim,
 631 Assaf Arbelle, Rameswar Panda, Rogerio Feris, and Zsolt Kira. Coda-prompt: Continual de-
 632 composed attention-based prompting for rehearsal-free continual learning. In *CVPR*, pp. 11909–
 633 11919, 2023.

634 Vishal Thengane, Salman Khan, Munawar Hayat, and Fahad Khan. Clip model is an efficient con-
 635 tinual learner. *arXiv:2210.03114*, 2022.

637 Liyuan Wang, Xingxing Zhang, Hang Su, and Jun Zhu. A comprehensive survey of continual
 638 learning: Theory, method and application. *IEEE TPAMI*, 46(8):5362–5383, 2024a.

639 Xi Wang, Xu Yang, Jie Yin, Kun Wei, and Cheng Deng. Long-tail class incremental learning via
 640 independent sub-prototype construction. In *CVPR*, pp. 28598–28607, June 2024b.

642 Zifeng Wang, Zizhao Zhang, Sayna Ebrahimi, Ruoxi Sun, Han Zhang, Chen-Yu Lee, Xiaoqi Ren,
 643 Guolong Su, Vincent Perot, Jennifer Dy, et al. Dualprompt: Complementary prompting for
 644 rehearsal-free continual learning. *ECCV*, 2022a.

646 Zifeng Wang, Zizhao Zhang, Chen-Yu Lee, Han Zhang, Ruoxi Sun, Xiaoqi Ren, Guolong Su, Vin-
 647 cent Perot, Jennifer Dy, and Tomas Pfister. Learning to prompt for continual learning. In *CVPR*,
 pp. 139–149, 2022b.

648 Yichen Wu, Hongming Piao, Long-Kai Huang, Renzhen Wang, Wanhua Li, Hanspeter Pfister, Deyu
649 Meng, Kede Ma, and Ying Wei. SD-loRA: Scalable decoupled low-rank adaptation for class
650 incremental learning. In *ICLR*, 2025.

651

652 Yue Wu, Yinpeng Chen, Lijuan Wang, Yuancheng Ye, Zicheng Liu, Yandong Guo, and Yun Fu.
653 Large scale incremental learning. In *CVPR*, pp. 374–382, 2019.

654

655 Guojun Yin, Bin Liu, Lu Sheng, Nenghai Yu, Xiaogang Wang, and Jing Shao. Semantics disen-
656 tangling for text-to-image generation. In *Proceedings of the IEEE/CVF conference on computer*
657 *vision and pattern recognition*, pp. 2327–2336, 2019.

658

659 Jiazu Yu, Yunzhi Zhuge, Lu Zhang, Ping Hu, Dong Wang, Huchuan Lu, and You He. Boost-
660 ing continual learning of vision-language models via mixture-of-experts adapters. In *CVPR*, pp.
661 23219–23230, 2024.

662 Friedemann Zenke, Ben Poole, and Surya Ganguli. Continual learning through synaptic intelligence.
663 In *ICML*, pp. 3987–3995. PMLR, 2017.

664 Yifan Zhang, Bingyi Kang, Bryan Hooi, Shuicheng Yan, and Jiashi Feng. Deep long-tailed learning:
665 A survey. *IEEE TPAMI*, 45(9):10795–10816, 2023.

666 Zangwei Zheng, Mingyuan Ma, Kai Wang, Ziheng Qin, Xiangyu Yue, and Yang You. Preventing
667 zero-shot transfer degradation in continual learning of vision-language models. In *ICCV*, pp.
668 19068–19079, 2023.

669

670 Zhisheng Zhong, Jiequan Cui, Shu Liu, and Jiaya Jia. Improving calibration for long-tailed recog-
671 nition. In *CVPR*, pp. 16489–16498, 2021.

672 Boyan Zhou, Quan Cui, Xiu-Shen Wei, and Zhao-Min Chen. BBN: Bilateral-branch network with
673 cumulative learning for long-tailed visual recognition. In *CVPR*, pp. 9719–9728, 2020.

674

675

676

677

678

679

680

681

682

683

684

685

686

687

688

689

690

691

692

693

694

695

696

697

698

699

700

701

702 APPENDIX: LEARNING FAST AND SLOW: ADDRESSING TASK-IMBALANCED
 703 CONTINUAL LEARNING WITH DECOUPLED DUAL-SPEED ADAPTATION
 704

705 A DETAIL PROOF OF THEOREM 1
 706

707 *Proof.* Let g_θ denote the text encoder and f_ϕ the image encoder. Denote the loss function over a
 708 task by $\mathcal{L}(f_\phi, g_\theta)$.

710 **Optimization landscape.** Text inputs are typically lower-dimensional, more structured, and carry
 711 strong semantic correlations. Image inputs are high-dimensional and more complex, with diverse
 712 patterns and noise. Thus, the Hessian $\nabla_\theta^2 \mathcal{L}$ for the text encoder tends to have larger eigenvalues
 713 along informative directions, leading to faster gradient descent convergence.

714 **Convergence rate comparison.** Using standard gradient descent with learning rate η :

$$\theta_{t+1} = \theta_t - \eta \nabla_\theta \mathcal{L}(\theta_t, \phi_t), \quad \phi_{t+1} = \phi_t - \eta \nabla_\phi \mathcal{L}(\theta_t, \phi_t),$$

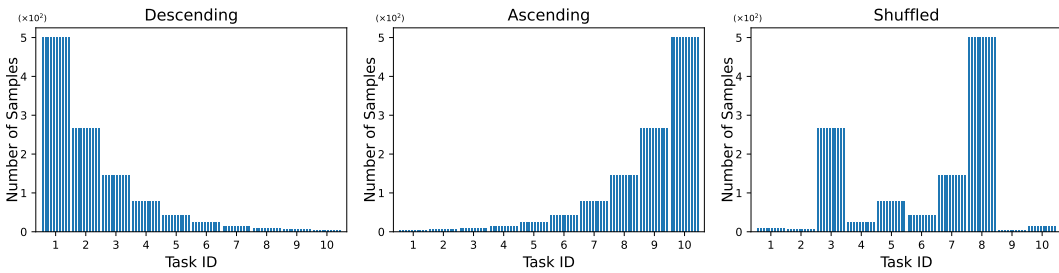
715 the text encoder updates θ converge faster because:

716 1. Smaller input dimension \Rightarrow fewer parameters and smoother loss landscape;
 717 2. Semantically structured inputs \Rightarrow gradients are more informative and less noisy;
 718 3. Fewer conflicting updates across classes.

719 **Implication for continual learning.** Once g_θ (text encoder) is near convergence, it serves as a stable
 720 semantic anchor. Subsequent updates of f_ϕ (image encoder) are guided to align with g_θ , stabilizing
 721 class-wise representations and mitigating feature drift and forgetting. \square

722 B VISUALIZATION OF DATA DISTRIBUTION UNDER TICL
 723

724 Figure A1 depicts the data distribution under the TICL setting (Hong et al., 2024), exemplified by
 725 CIFAR100-TICL. The task sizes follow a long-tailed distribution, whereas the categories within
 726 each task are balanced.



727 Figure A1: Illustration of the data distribution in CIFAR100-TICL. (The categories within each task
 728 can be clearly visible upon magnification.)

729 C SEQUENTIAL TASK PERFORMANCE ON CIFAR100-TICL AND
 730 TINYIMAGENET-TICL

731 Figure A2 (in Page 15) compares the average accuracy across all encountered tasks. DFSA
 732 consistently demonstrates robust performance. Notably, even when compared against methods pre-
 733 trained on ImageNet-21K, which has overlap with the training data, DFSA outperforms some of
 734 these methods in the more challenging Ascending scenario (Figure A2a), showing its effectiveness
 735 under extreme task imbalance and limited early data.

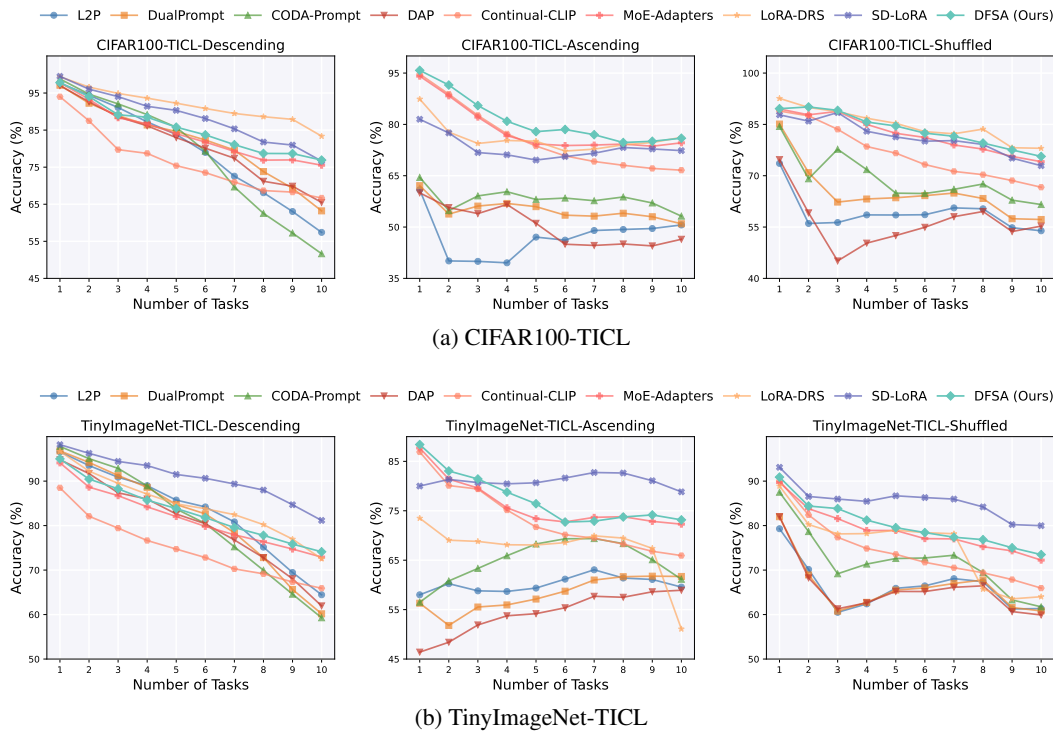
736 D PER-TASK PERFORMANCE COMPARISON

737 Figure A3a (in Page 16) shows the per-task accuracy after learning the final task for methods using
 738 linear classifiers. It can be seen that task performance is highly sensitive to data volume, with

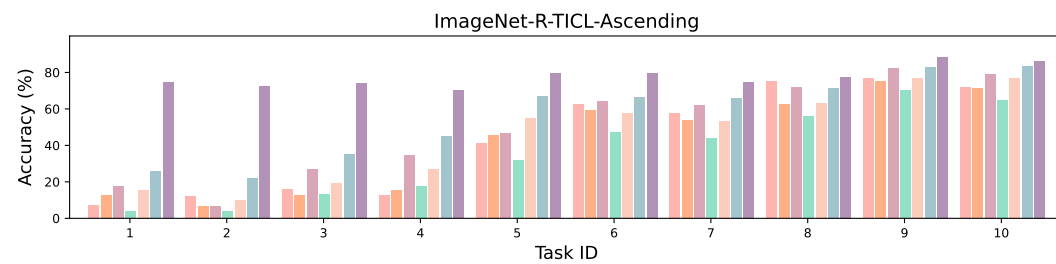
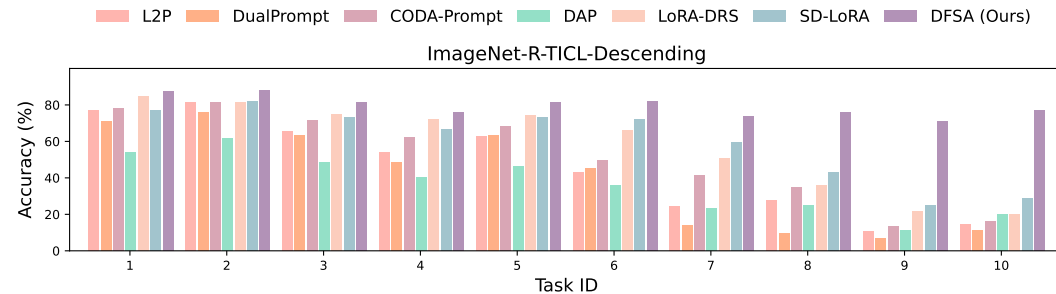
756 data-scarce tasks exhibiting extremely poor accuracy. In contrast, our DFSA maintains consistently
 757 strong performance across all tasks, demonstrating its stability in task-imbalanced continual learning
 758 and its effectiveness in mitigating both the stability–plasticity and head–tail learning dilemmas.
 759 Similarly, Figure A3b compares DFSA with textual classifier methods, namely Continual-CLIP
 760 and MoE-Adapters. While all methods leverage textual information to reduce sensitivity to data
 761 scarcity, DFSA achieves higher accuracy on more tasks, further showing its robustness under long-
 762 tailed incremental scenarios.

764 DISCLOSURE OF LLM USAGE

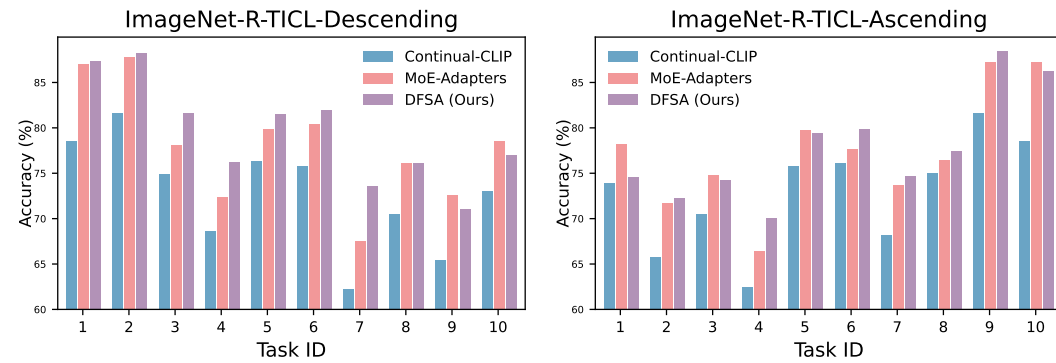
766 In accordance with the ICLR 2026 policy, we disclose that large language models (e.g., ChatGPT,
 767 Deepseek) were used only to aid in the polishing of grammar and phrasing. Their usage was strictly
 768 limited to improving readability and presentation. They were not used for research ideation, method-
 769 ology design, algorithm development, data collection, data analysis, experimental design, result
 770 interpretation, or any aspect related to the originality and technical contributions. All scientific
 771 contributions are original to the authors.



796 Figure A2: Average accuracy on all encountered tasks after sequential training on (a) CIFAR100-
 797 TICL, and (b) TinyImageNet-TICL.



(a) Per-Task Comparison with Linear Classifier Methods



(b) Per-Task Comparison with Other Textual Classifier Methods

Figure A3: Per-task performance comparison after training final task: (a) our DFSA vs. linear classifier methods, and (b) our DFSA vs. textual classifier methods.